RADAR IMAGING OF MERCURY'S NORTH AND SOUTH POLES AT 3.5 CM WAVELENGTH. L.J. Harcke, H.A. Zebker, *Dept. of Electrical Engineering, Stanford University, Stanford, CA 94305-9515 (lharcke@stanford.edu)*, R.F. Jurgens, M.A. Slade, *Jet Propulsion Laboratory, California Inst. of Technology, Pasadena, CA 91109-8099*.

The Goldstone Solar System Radar has been used to image the north and south poles of Mercury during the inferior conjunctions of February 2001 and June 2001. The sub-Earth latitude was -10.7° in February during observations of the southern hemisphere, and $+8.4^\circ$ in June during observations of the northern hemisphere. These excellent viewing angles provided an opportunity to resolve the radar bright material in polar craters at 6 km range resolution. Fine-scale (1.5 km) resolution images of the northern craters have previously been obtained at 13 cm wavelengths during the July 1999 inferior conjunction (Harmon et al., 2001). However, due to geometric constraints, the Arecibo radar cannot observe the southern polar region of Mercury until 2004. Our new Goldstone 6 km data are a factor of two higher resolution than Arecibo data collected in March 1992 at 15 km range resolution (Harmon et al. 1994), and will remain the most highly resolved images of the south polar region for the next few years.

The long-code method of delay-Doppler mapping (Harmon et al., 1992) was used to prevent aliasing of the radar return, as Mercury is nearly 5 times overspread at 3.5 cm. The radar transmitted RC polarization and received both RC and LC polarizations. Several transmit-receive cycles were averaged in delay-Doppler space to obtain the images in Figures 1 (4 cycles averaged) and 2 (10 cycles averaged). In these delay-Doppler space images, the pole appears near the center of the image, as the projection into radar coordinates approximates a polar stereographic projection. The hemisphere opposite the sub-Earth point lies in radar shadow, and does not appear in the picture. The standard north-south ambiguity of delay-Doppler mapping does not affect observations of the polar region at these viewing geometries, as the corresponding points at the opposite pole lie in radar shadow. Only data from the same circular (SC) polarization as transmitted are shown, as the strong specular reflection in the OC data from the sub-radar point lowers the overall contrast of the image and masks the polar return.

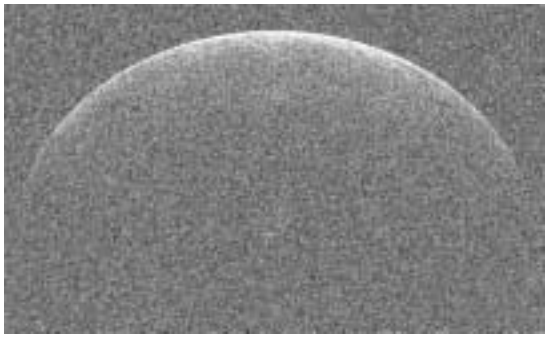

Figure 1: Mercury north hemisphere 2001 June 13

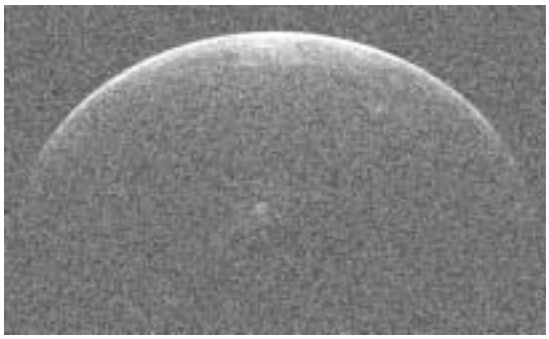

Figure 2: Mercury south hemisphere 2001 Feb. 20

The north polar craters (Figure 3) exhibit brightest reflections from material at their southern rims as noted previously (Harmon et al., 2001; Slade et. al, 2000), which are the areas that are permanently in shadow from the Sun. The south polar scene (Figure 4) is dominated by the reflection from the Chao Meng-Fu crater, though bright reflection from numerous smaller craters can be seen. The brightness of these features is consistent with volume scattering from cold-trapped volatiles. Similar radar bright echo and polarization inversion (SC stronger than OC) has been noted for the Galilean satellites since the mid 1970's (Campbell et al., 1978), and is usually explained using models of coherent backscatter from icy media (Hapke, 1990). Comparison of the radar albedo at the Arecibo

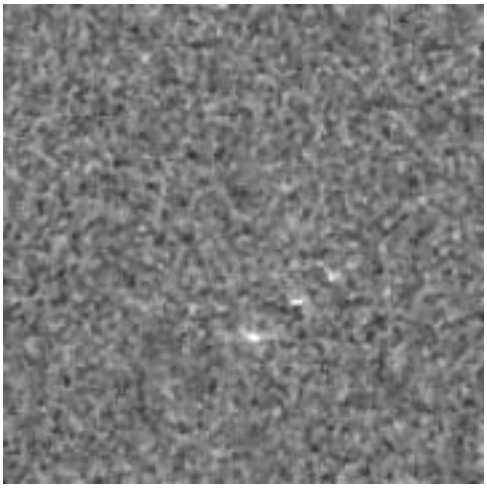

Figure 3: Mercury north pole 2001 June 13

and Goldstone wavelengths has the potential to constrain scattering mechanisms, and lead to a better understanding of the environment in and around the crater which allows the volatiles to become trapped.

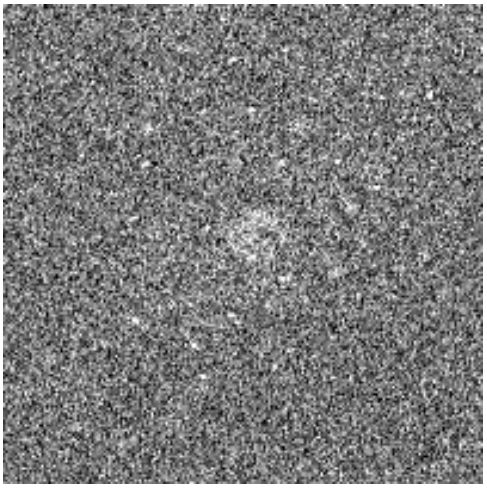

Figure 4: Mercury south pole 2001 Feb. 20

Campbell, D.B. et al. (1978). *Icarus*, **34**, 254.
Harmon, J.K. et al. (1992). *Icarus*, **95**, 153.
Harmon, J.K. et al. (1994). *Nature*, **369**, 213.
Harmon, J.K. et al. (2001). *Icarus*, **149**, 1.
Hapke, B. (1990). *Icarus*, **88**, 407.
Slade, M.A. et al. (2000). *31st LPSC*, abstract 1305.